

Proline-40 is Essential to Maintaining Cytochrome b_5 's Stability and Its Electron Transfer with Cytochrome c [†]

WANG, Zhi-Qiang^{1,a}(王志强) WU, Jian^{1,c}(邬建) WANG, Yun-Hua^a(王韵华)
QIAN, Wen^a(钱雯) XIE, Yi^b(谢毅) XIA, Zong-Xiang^{*,c}(夏宗芾)
HUANG, Zhong-Xian^{*,a}(黄仲贤)

^a Chemical Biology Laboratory, Chemistry Department, Fudan University, Shanghai 200433, China

^b National Key Lab of Genetics, Fudan University, Shanghai 200433, China

^c State Key Laboratory of Bioorganic and Natural Products Chemistry, Shanghai Institute of Organic Chemistry, Chinese Academy of Sciences, Shanghai 200032, China

In order to illustrate the roles played by Pro40 in the structure, properties and functions of Cytochrome b_5 , three mutated genes, P40V, P40Y, P40G were constructed in this work. Only the P40V gene was successfully expressed into holoprotein in *E. coli* JM83. According to the results of X-ray crystallographic analysis and various kinds of spectroscopy studies, it is evident that substituting valine for Pro40 does not result in significant alterations in the protein's overall structure; however, local conformational perturbations in the proximity of the heme do occur. The redox potential of the P40V mutant is 40 mV lower than that of the wild type protein. Its stability towards heat, urea, acid and ethanol were significantly decreased. The mutation leads to a decrease in the hydrophobicity of the heme pocket, which is probably the major factor contributing to the above changes. Binding constants and electron transfer rates between cytochrome b_5 and cytochrome c were determined using UV-visible spectroscopy and stopped-flow techniques for both the wild type and the mutant. The results showed that the substitution of Pro40 by valine does not influence the binding constant of cytochrome b_5 to cytochrome c ; however, the electron transfer rate between them decreased significantly. This indicates that proline-40 is essential to maintaining cytochrome b_5 's stability and its electron transfer with cytochrome c . These studies also provided a good example that property and functional changes of a protein do not necessarily require large overall structural alterations; in most cases, only perturbations on the local conformations are sufficient to induce significant

changes in protein's properties and functions.

Keywords cytochrome b_5 , mutation, stability, function, X-ray structure analysis

Introduction

Cytochrome b_5 (Cyt b_5) is a membrane-bound protein. It can be proteolyzed to yield a soluble, hydrophilic domain containing a non-covalently bound heme group. Cyt b_5 is involved in electron transfer with a variety of proteins, such as cytochrome c (Cyt c),¹⁻³ metmyoglobin,² methemoglobin,⁴ and cytochrome $P450$.^{5,6} In 1981, Bernardi and Azzone⁷ presented evidence that *in vivo*, Cyt c can function as an efficient electron shuttle between a form of Cyt b_5 , existing in the outer mitochondria membrane,⁸ and cytochrome c oxidase. Owing to the availability of the detailed structures and the easy preparation of these two proteins, interactions between Cyt b_5 and Cyt c serve as models for the electron transfer between macromolecules in general. It is proposed that the electrostatic interactions between negatively charged residues of Cyt b_5 (including glutamates surrounding the exposed heme edge and heme propionate group) and posi-

* E-mail: zxhuang@fudan.edu.cn; xiazx@pub.sioc.ac.cn [†]The two authors made equal contributions to this work.

Received May 6, 2002; revised and accepted July 12, 2002.

Project supported by the National Natural Science Foundation of China (Nos. 39990600 and 20071009), and the State Key Laboratories of Genetic Engineering of School of Life Science of Fudan University.

[†]Dedicated to Professor HUANG Yao-Zeng on the occasion of his 90th birthday.

tively charged residues (mainly lysine residues) of Cyt *c* help to steer the two proteins to form a transient complex prior to electron transfer.^{9,10,11}

Proline-40, one of the hydrophobic patch residues on the surface of Cyt *b*₅ and also a member of the heme hydrophobic pocket residues, makes close contacts with the heme prosthetic group by van der Waals interactions.^{11,12} This residue is an invariant residue among different species of Cyt *b*₅ in biology.¹³ In addition, Pro40 locates at the position adjacent to His39, one of the axial ligands of heme iron, forming an aromatic ring channel with Tyr74 and His39 residues. It is also noted that Pro40 is at the β -turn between α -helix II (residues 30–39) and α -helix III (residues 42–49), and makes a sharp γ -bend of the polypeptide chain (Fig. 1). Its five-atom ring might serve as a restriction factor in the structure and folding of the polypeptide chain. It would be expected that Pro40 would play a unique structural role in modulating the strength of the closed crevice of Cyt *b*₅. In an attempt to investigate the roles played by this invariant

residue, three mutant genes, P40V, P40G and P40Y were constructed for this work. Only the P40V gene has been successfully expressed into holoprotein. The fundamental properties and structure of this mutated protein have been characterized by electrospray-mass spectrometry, electrochemical and spectroscopic measurements, and X-ray crystallographic analysis. Its stability towards heat, urea, acid and ethanol has been investigated. Furthermore, the binding constants and electron transfer properties of the mutant and wild type Cyt *b*₅ with Cyt *c* have been measured by means of UV-visible difference spectra and stopped-flow techniques. The X-ray structural analysis shows that elimination of the rigid five-member ring after mutation of proline by valine has not made significant overall structural alteration of the protein; only the local structural changes have been observed. However, the protein stability, properties and electron transfer reaction rates have been greatly affected.

Materials and methods

General materials

The pUC19 plasmid containing the synthesized gene coding for the trypsin-solubilised bovine liver Cyt *b*₅ (82 residues in length) was a kind gift from Professor A. Mauk.¹⁴ DNA restriction endonucleases, polymerases, ligases, and kinases were purchased from Pharmacia or Promega. Proflavine hemisulfate and methylviologen were purchased from Tokyo Chemical Industry Co. Ltd. All other chemicals used were of analytical grade.

Protein preparation

The site-directed mutagenesis of the gene encoding Cyt *b*₅ was performed as described by Zoller and Smith.¹⁵ Three 21-base oligonucleotides were synthesized and purified. The codon of Pro40 (CCG) was changed to GTA (Val), TAT (Tyr) and GGC (Gly), respectively. The mutated genes were ligated into *EcoR* I/*Hind* III cut pUC19 plasmid and transformed into *E. coli* JM83. The expression and purification of the mutants were performed according to the literature.¹⁴ Electrospray mass spectrometry (ES-MS) was used to measure the molecular weight of the mutant protein. The redox potential was measured by differential pulse voltammetry (DPV) as described in the literature.¹⁶

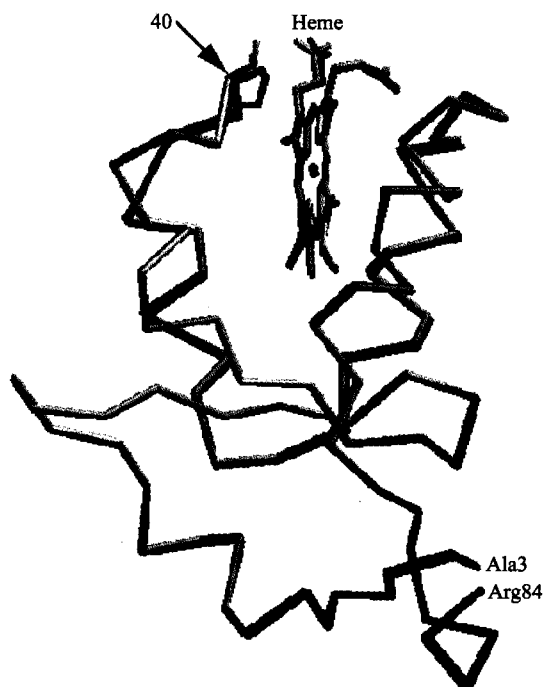


Fig. 1 Stereoscopic α drawing of Cyt *b*₅ P40V mutant, superimposed with those of wild type Cyt *b*₅. The heme and the side chains of Val40/Pro40 are also shown. Cyt *b*₅ P40V is shown in thin lines and wild type Cyt *b*₅ in thick lines (PDB access 1M59 for the P40V mutant).

X-Ray crystallographic analysis of the P40V mutant

The single crystals of the P40V mutant of trypsin-solubilised cytochrome *b*₅, Cyt *Tb*₅ P40V mutant were grown in hanging drops of 5 μ L of the protein solution (20 mg/mL) mixed with 5 μ L of the reservoir solution (2.6–2.7 mol/L phosphate buffer, pH 8.0) at 20 °C, which is similar to the crystallization conditions of both trypsin- and lipase-solubilised wild type cytochrome *b*₅, Cyt *Tb*₅¹² and Cyt *Lb*₅¹⁷. The crystals belong to the monoclinic space group *C2*, which is the same as that of wild type Cyt *b*₅ crystals,¹² but the unit cell parameters, *a*, *c* and β are slightly larger than those of Cyt *b*₅. The crystal data of the P40V mutant compared with those of wild type Cyt *b*₅ are listed in Table 1.

Table 1 Crystal data of the P40V mutant compared with those of wild type Cyt *Tb*₅

	P40V	<i>b</i> ₅ (WT)
Space group	<i>C2</i>	<i>C2</i>
Cell dimensions		
<i>a</i> (nm)	7.096	7.070
<i>b</i> (nm)	4.038	4.044
<i>c</i> (nm)	3.943	3.928
β (°)	112.33	111.76
Number of molecules per asymmetric unit	1	1
V_m (nm ³ /Da)	0.00277	0.00261

The X-ray data were collected up to 0.19 nm resolution using one crystal on the MarResearch Imaging Plate-300 Detector System. The data were processed using the program DENZO and SCALEPACK,¹⁸ giving an R_{sym} of 0.053 and the data completeness of 93.7%. Table 2 summarizes the data collection statistics.

The determination and the refinement of the P40V mutant structure were carried out using the program package X-PLOR on a Silicon Graphics Indigo2 workstation.¹⁹ The model building was performed using the graphics software TURBO-FROO.²⁰ The initial structural model of the P40V mutant was determined using the difference Fourier method based on the crystal structure of the Cyt *b*₅ F35Y mutant refined at 0.18 nm resolution.²¹ The rigid body refinement was carried out, and at this stage the data were limited to 0.22 nm resolution. The structure was further refined for both atomic positions and temperature factors for a number of rounds. The side chain of Val40 was fitted to the electron density, and the model was im-

proved by using the $(2F_o - F_c)$ and the $(F_o - F_c)$ electron density maps calculated regularly. The simulated annealing "omit" maps were calculated as well when necessary. During the refinement, the resolution was gradually extended to the highest value 0.19 nm, and the solvent molecules were gradually fitted.

Table 2 Data collection statistics of Cyt *b*₅ P40V mutant

Highest resolution (nm)	0.190
Number of unique reflections	7747
R_{linear} (%) ^a	5.3 (19.4) ^b
Data completeness (%)	93.7 (91.8) ^b
$\langle I/\sigma(I) \rangle$ ^c	21.1 (7.9) ^b

^a $R_{\text{linear}} = \text{SUM}(\text{ABS}(I - \langle I \rangle)) / \text{SUM}(I)$. ^bThe numbers in the parentheses correspond to the data in the highest resolution shell (0.190–0.194 nm). ^cMean signal-to-noise ratio.

The more powerful program package CNS²² was used to further refine the structure. The simulated annealing procedure starts from 2500 K with a cooling rate of 25 K per cycle, followed by the individual B refinement. Simulated annealing "omit" map was calculated in order to verify the side chain conformation of Val40.

Stability study of the mutant protein

The denaturation of Cyt *b*₅ P40V mutant by thermal, urea, ethanol and acid were employed as described previously.^{23,24} The proteins were dissolved in 100 mmol/L sodium phosphate buffer (pH 7.0) or 100 mmol/L potassium acetate buffer (pH = 1.2–5.3) with a concentration of 5 μ mol/L. The concentrations of Cyt *b*₅ and its mutants were determined using $\epsilon_{412 \text{ nm}} = 117000 \text{ mol}^{-1} \cdot \text{L} \cdot \text{cm}^{-1}$.²⁵

*Binding and electron transfer between cytochrome *b*₅ and cytochrome *c**

UV-visible difference spectra of the proteins were recorded using a matched mixing cell. The K_A was determined as described.¹ The concentration of Cyt *c* was determined on the basis of $\epsilon_{410 \text{ nm}} = 106100 \text{ mol}^{-1} \cdot \text{L} \cdot \text{cm}^{-1}$.²⁶

Rapid mixing experiments were performed with a computer-controlled Hi-Tech SF-61 DX2 Double-Mixing Stopped-flow Spectrophotometer (Hi-Tech Scientific Ltd., U.K.). The electron transfer rates were obtained

as described.²⁷

Results

Mutagenesis, expression and purification of cytochrome b_5

The mutated genes, P40V, P40Y and P40G were obtained by means of site-directed mutagenesis, and were cloned into the pUC19 vectors, and then transformed into *E. coli* JM83 as described in Methods. Replacement of Pro40 with a valine yielded red color cells which contained the mutant protein. However, the P40Y and P40G genes cannot be expressed into the corresponding holoprotein in this system, suggesting that the mutated proteins are not stable. The yield of the purified protein of P40V was 4 mg per liter of culture solution, which is nearly one fourth of yield of the wild type protein. The purified protein showed a single band on SDS-PAGE. The molecular weight determined by ESI-MS is 9464.7 ± 2.2 , which agrees well with the calculated value of 9463.3. These results confirmed the successful mutagenesis.

General properties of the mutant protein

In order to illustrate the role played by Pro40 in the structure and functions of Cyt b_5 , the purified P40V mutant protein have been characterized. UV-visible spectroscopy, circular dichroism of the P40V mutant protein, and the fluorescence spectrum of apo-P40V (Cyt b_5 P40V with the heme removed) indicate that spectroscopic features of the mutant are practically identical to those of the corresponding wild-type protein. Thus, the ligation environment of the heme and microenvironment that includes the aromatic amino acids, tyrosine and tryptophan, did not change significantly by the mutation. These results reveal that the substitution of Pro40 to valine did not result in a significant change of the overall structure of the protein.

Cyt b_5 is an electron-transfer protein. Its redox potential (~ 5 mV vs. NHE) can be regarded as the driving force for the biochemical reactions. It is notable that the redox potential of the P40V mutant is approximately 40 mV lower than that of the wild type protein.

Crystal structure of cytochrome b_5 P40V mutant

The P40V mutant structure that was refined at 0.19

nm resolution gave an R factor of 0.193 and an R_{free} of 0.227, respectively. The r.m.s. deviations of the bond lengths and bond angles from the ideal values are 0.0010 nm and 1.11° , respectively. Table 3 shows the refinement statistics.

Table 3 Refinement statistics of Cyt b_5 P40V mutant

No. of amino acid residues	82
No. of prosthetic group	1
No. of solvent molecules	93
R -factor (%)	19.3
Free R -factor (%)	22.7
r.m.s.d. ^a	
Bond lengths (nm)	0.0010
Bond angles ($^\circ$)	1.11
Mean temperature factors (nm^2)	
Main chain	0.1972
Side chain	0.2370
Heme	0.2190
Solvent	0.4005

^a Root-mean-square deviation.

The Ramachandran plot²⁸ of the final model shows that all of the non-glycine residues are located within the acceptable regions, with 91.8% in the most favored region obtained by running the program PROCHECK^[31]. The Luzzati plot shows that the estimated error of the atomic coordinates is approximately 0.022 nm.²⁹

The overall structure of the P40V mutant is similar to that of wild type Cyt b_5 . Fig. 1 shows the superimposed $C\alpha$ backbone of the two molecules. The r.m.s. deviation of the coordinates of the $C\alpha$ atoms between the two molecules is 0.012 nm. The secondary structure of the P40V mutant is essentially identical to that of Cyt b_5 .¹² The residue Pro40 is located in the β -turn of His39-Gly42 between helix II and helix III, and it was expected to play an important role in the folding of the polypeptide chain because proline is a residue favorable to form β -turn. However, the structure of the P40V mutant shows that the mutation from the invariant proline to valine does not eliminate this β -turn, but only results in change of the local conformation of the polypeptide chain. The $C\alpha$ atom deviation of this residue between the P40V mutant and wild type Cyt b_5 structures is 0.040 nm when they are superimposed. The atom $C\beta$ of the side chain of Val40 in the P40V mutant points toward the top of the heme pocket, and makes van der Waals contacts to the heme with the shortest distance of 0.418 nm from the atom $C\beta$ of Val40 to the carbon atom C2A of the pyrrole group of the heme (Fig. 1).

The conformation of the heme in the P40V mutant is very similar to that of Cyt b_5 . One of the heme propionates is hydrogen-bonded to the main chain and to the side chain atoms of Ser64, which displays the conserved conformation in Cyt b_5 and its mutants.^{12,16,21} The other propionate group extends into the aqueous environment and does not form any hydrogen bonds with protein atoms. However, the latter propionate group adopts the slightly different conformations in various mutant protein structures. The coordination distances between Fe and NE2 atoms of His39 and His63 are 0.209 nm and 0.205 nm, respectively, which are almost the same as those in the wild type Cyt b_5 ¹² and in the V61H mutant structures.¹⁶

A water molecule, Wat321, with low temperature factor (0.227 nm^2) was found near the mutation site in the P40V mutant structure. It forms three hydrogen bonds; one to the main chain nitrogen atom of Val40, a second to the main chain oxygen atom of Glu38, and the third to a water molecule (Wat322) of a symmetry-related molecule (Fig. 2). Wat321 does not exist in wild type

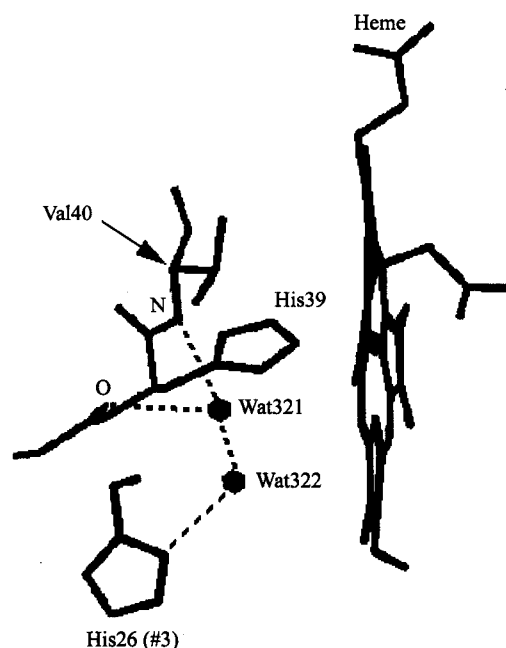


Fig. 2 Hydrogen bond network near the mutation site in the heme pocket of Cyt b_5 P40V mutant. This network involves Val40, Glu38, and Wat321 of the molecule at XYZ , as well as His26 and Wat322 of the symmetry-related molecule at $-X + 1/2 Y + 1/2 - Z$ (#3). N and O denote the main chain nitrogen atom of Val40 and the main chain oxygen atom of Glu38. The hydrogen bonds are shown in dashed line.

Cyt b_5 or in other mutants,^{12,16} while Wat322 is a conserved water molecule and is hydrogen bonded to the side chain of His26 as well as another water molecule of a symmetry-related molecule. This hydrogen bond network probably helps stabilize the crystal structure of the mutant.

Protein stability

Thermal stability studies Fig. 3a describes the changes in the absorption spectrum of the P40V mutant upon exposure to increasing temperature. The maximum absorbance of Soret band for the oxidized form is at 412 nm. As shown in Fig. 3a, with increasing temperature, the absorbance of Soret band decreases significantly and is shifted to shorter wavelengths with an isosbestic point at 392 nm. Previous studies have established that heat denaturation of Cyt b_5 can be generally analyzed in terms of a two-state mechanism,³⁰⁻³³ though some complicated processes have been mentioned in the kinetics of Cyt b_5 denaturation.³⁴ Normalized absorbance as a function of temperature is shown in Fig. 3b for both the wild type protein and the P40V mutant. According to this curve the transition temperature (T_m) can be estimated. We have also investigated the heat stability of the corresponding reduced protein. Similar results were obtained (Fig. 3c). Thermodynamic data are listed in Table 4. Based on these values, it is obvious that ferrocycytochrome b_5 of the wild type and the mutant are significantly more stable towards heat than the corresponding ferricytochrome b_5 . Furthermore, it can be seen that for both the oxidized and the reduced forms of P40V, the midpoint temperatures of transition are about 8.6 and 11.5 °C lower than those for the corresponding wild type proteins (Table 4). This result clearly indicates that the substitution of Pro40 by valine leads to the mutant protein less stable than the wild type protein.

Urea denaturation Absorption spectra of the denaturation of the mutant and wild type Cyt b_5 induced by urea changed in the same way as those of heat denaturation. Fig. 4 shows the normalized absorbance of wild type Cyt b_5 and the P40V mutant upon exposure to increasing concentrations of urea. In the case of the P40V mutant, the midpoint concentration of urea required to produce a half of unfolded protein (5.4 mol/L) is lower than that of the wild type protein (6.8 mol/L). Table 5 gives the thermodynamic parameters of urea denaturation. Substitution of the invariant Pro40 was shown to decrease the sta-

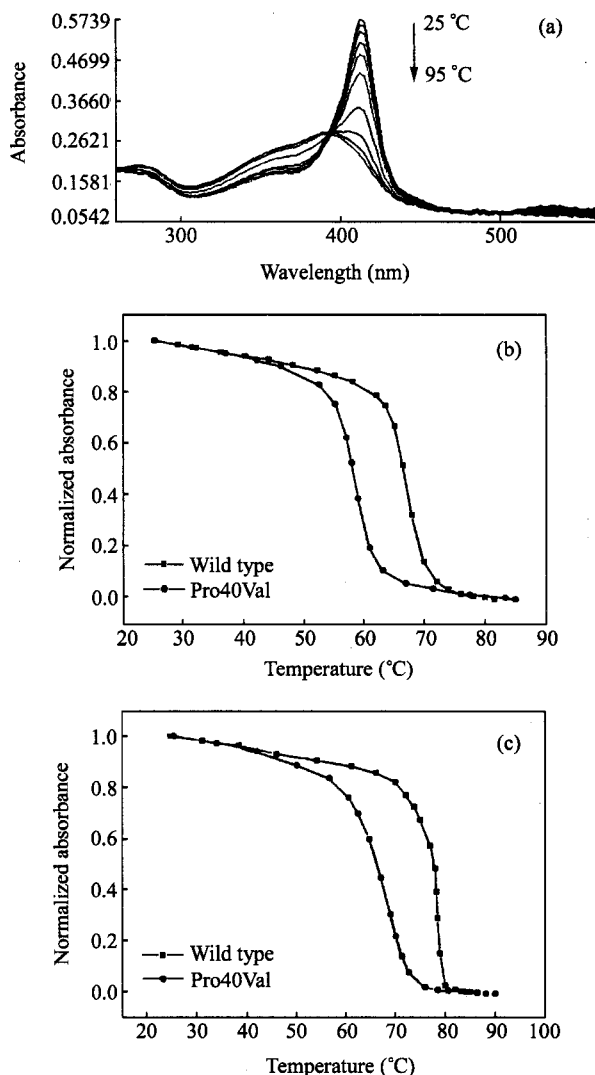


Fig. 3 Equilibrium studies of thermal denaturation of the wild type and P40V mutant of Cyt b_5 . (a) Absorbance spectra of the ferricytochrome b_5 P40V at temperatures of 28.2, 36.8, 46.0, 52.4, 55.1, 57.0, 59.0, 61.0, 63.2 and 67.0 °C. (b) Normalized changes in absorbance at 412 nm with increasing temperature for the oxidized proteins. (c) Normalized changes in absorbance at 424 nm with increasing temperature for the reduced proteins.

Table 4 Thermodynamic data for thermal denaturation of cytochrome b_5 ^a

Cytochrome b_5	T_m (°C)	ΔT_m (°C)	$\Delta(\Delta G_D^{50\%})$ (kJ/mol)
Oxidized WT	66.7	—	—
Oxidized P40V	58.1	-8.6	-10.0
Reduced WT	77.6	—	—
Reduced P40V	66.1	-11.5	-12.5

^a 100 mmol/L sodium phosphate buffer, pH 7.0.

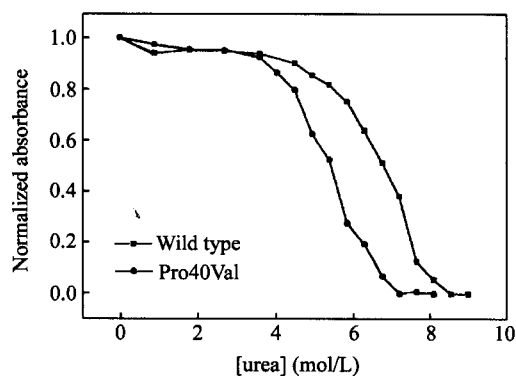


Fig. 4 Normalized changes in absorbance of the wild type and the P40V mutant of cytochrome b_5 measured at 412 nm as a function of the urea concentration.

bility by 5.3 kJ/mol. The K_D of the P40V mutant is 8.8 fold larger than that of the wild type, indicating that the peptide chain in the mutant binds heme about 9-fold less tightly than that in the wild type protein. Thus, the urea denaturation of the P40V mutant shows similar result that the mutant protein is less stable than the wild type protein.

Acid and ethanol denaturation The mechanisms of denaturation for Cyt b_5 towards acid and organic solvent are complicated. The profiles of absorption spectra are very different from those of spectra obtained from urea or heat denaturation. No isosbestic point is observed. The midpoints (where normalized absorbance equals to 0.5) of

Table 5 Urea denaturation of bovine cytochrome b_5 ^a

Cytochrome b_5	C_m (mol/L)	m_D (kJ·L/mol ²)	$\Delta(\Delta G_D^{50\%})$ (kJ/mol)	$K_D(\text{mutant})/$ $K_D(\text{WT})$
Wild Type	6.8	-3.7	—	—
P40V	5.4	-3.9	-5.3	8.8

^a 100 mmol/L sodium phosphate buffer, pH 7.0.

the P40V mutant and the wild type protein towards acid (Fig. 5) are pH 4.5 and pH 4.0, respectively. The midpoints of the changes in spectra of the proteins towards ethanol (Fig. 6) are 35% (WT) and 28% (P40V), respectively. In both cases, the P40V mutant was more susceptible to denaturants than the wild type protein.

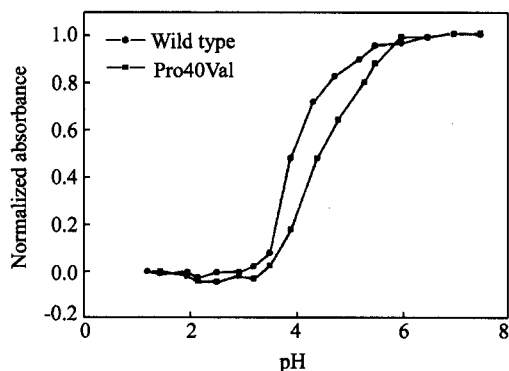


Fig. 5 Acid denaturation of the wild type and P40V mutant of cytochrome b_5 in various pH conditions monitored at 412 nm.

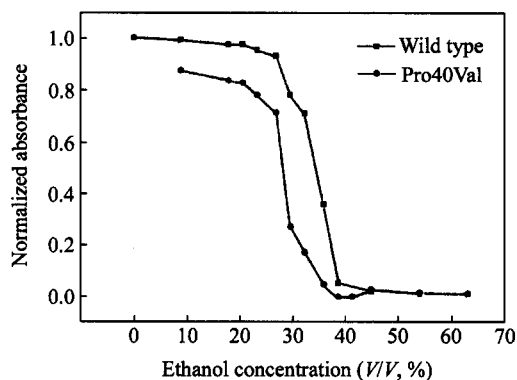


Fig. 6 Denaturation of the wild type and P40V mutant of cytochrome b_5 in different concentrations of ethanol monitored at 412 nm.

Binding and electron transfer between cytochrome b_5 or the P40V mutant and cytochrome c

Interactions between Cyt b_5 and Cyt c induce perturbations to the heme pocket of the proteins. This leads to changes in their absorption spectra of the heme center. The maximum in the difference spectrum occurs near 416 nm (Fig. 7a). When the concentration ratio of Cyt c to Cyt b_5 is increased, the maximum change in the absorbance at 416 nm increases until a 1:1 complex is

formed between Cyt c and Cyt b_5 (Fig. 7b). Many investigations have confirmed that Cyt b_5 and Cyt c form a 1:1 complex in solution. The titration data could be fit to the following equation according to the literature methods.³⁵

$$\Delta A = \Delta A_{\infty} / (2b) \times \{c + b + 1/K_A - [(c + b + 1/K_A)^2 - 4cb]^{1/2}\}$$

where ΔA is the change in absorbance of 416 nm upon complex formation, and b and c represent the total concentrations of Cyt b_5 and Cyt c , respectively. K_A is the equilibrium association constant. ΔA_{∞} is the absorbance at infinite Cyt c concentration. The K_A for the wild type protein was determined to be $(1.13 \pm 0.60) \times 10^6$ L/mol by non-linear regression fitting of the curves. This is consistent with the value reported in the literature.³⁶ Under the same conditions, the K_A for the P40V mutant was

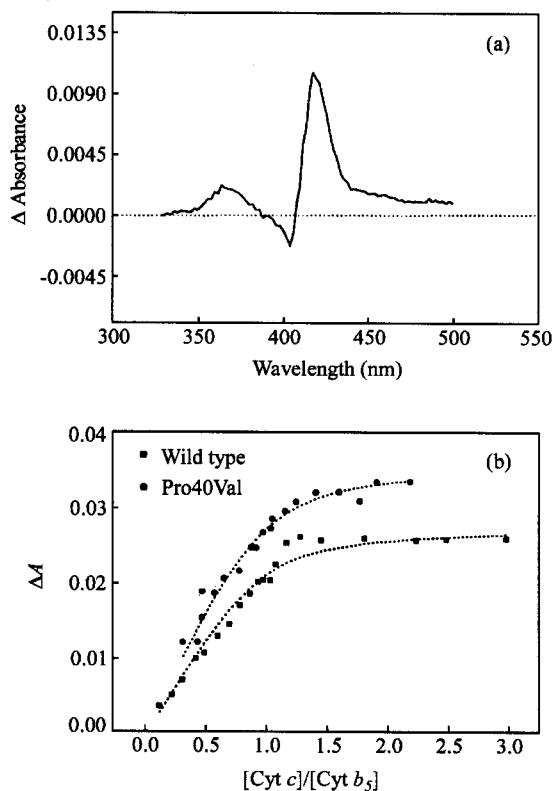


Fig. 7 (a) Difference spectrum due to complex formation in a solution containing 4.56 $\mu\text{mol/L}$ cytochrome c and 7.47 $\mu\text{mol/L}$ cytochrome b_5 (pH 7.0 phosphate buffer, $I = 1$ mmol/L, 25 $^{\circ}\text{C}$). (b) Spectrophotometric titration of cytochrome b_5 with increasing concentrations of cytochrome c .

found to be $(1.78 \pm 0.73) \times 10^6$ L/mol, suggesting that the substitution of proline does not affect the binding between the two proteins significantly.

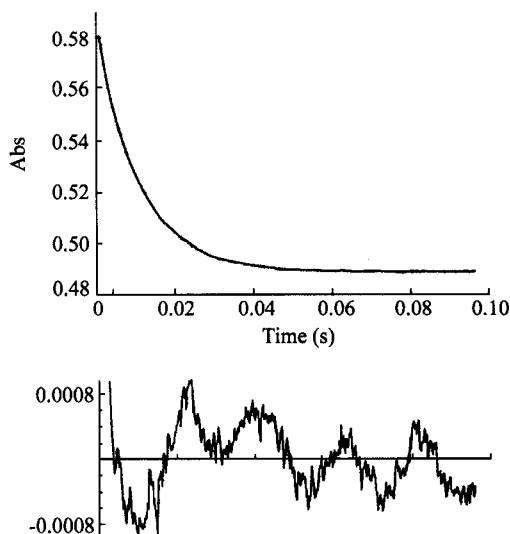


Fig. 8 Kinetic trace of reduction of ferricytochrome *c* by ferrocytochrome *b*₅. Experimental conditions: *I* = 150 mmol/L phosphate buffer (pH 7.0), 20.5 °C.

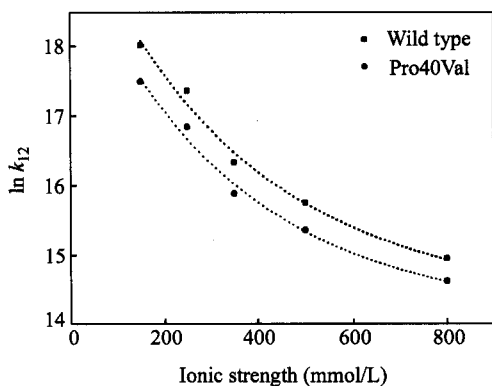


Fig. 9 Dependence of the bimolecular rate constant of the reduction of ferricytochrome *c* by wild type and mutant ferrocytochrome *b*₅ on ionic strength.

Kinetic studies of the reduction of ferri-Cyt *c* by ferro-Cyt *b*₅ were undertaken at different ionic strengths and various temperatures. Fig. 8 is a typical tracing curve of absorbance at 428 nm as a function of time. Electron transfer rate (k_{12}) was obtained by non-linear regression using routines in the Hi-Tech program. The second order rate constants for all redox reactions between ferri-Cyt *c* and ferro-Cyt *b*₅ are presented in Table 6. It is obvious that the rate constants decrease significantly with increas-

ing ionic strength. Furthermore, $\ln k_{12}$ was approximately exponentially related to ionic strength (Fig. 9). This suggests that electrostatic interactions play a significant role in the process of electron transfer.³ It can be seen from Table 6 that at all ionic strengths, electron transfer rates between the P40V mutant and Cyt *c* are slower than those of the wild type protein.

Table 6 Rate of electron transfer from ferrocytochrome *b*₅ to ferricytochrome *c* at various ionic strength^a

<i>I</i> (mmol/L)	WT	P40V
150	66.6 ± 2.3	39.2 ± 1.1
250	34.3 ± 1.4	20.5 ± 1.6
350	12.4 ± 0.2	7.9 ± 0.5
500	6.9 ± 0.1	4.7 ± 0.1
800	3.1 ± 0.2	2.2 ± 0.1

^aAll rates are given in unit of $10^6 \text{ mol}^{-1} \cdot \text{L} \cdot \text{s}^{-1}$. Experimental conditions are 20 °C, phosphate buffer (pH 7.0).

Electron transfer rates between ferro-Cyt *b*₅ and ferri-Cyt *c* become faster with increasing temperature. Fig. 10 shows the temperature dependence of electron transfer rate constant at ionic strength of 150 mmol/L. The activation entropy (ΔS^\ddagger) and enthalpy (ΔH^\ddagger) were obtained from linear regression analysis and are presented in Table 7.

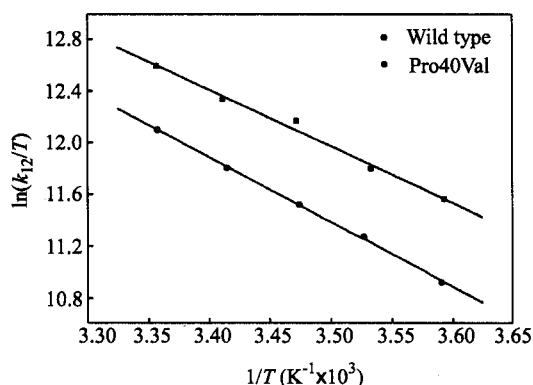


Fig. 10 Eyring plots of the rate constant of ferricytochrome *c* reduction by wild type and mutant ferrocytochrome *b*₅ (*I* = 150 mmol/L, pH 7.0 phosphate buffer).

Discussion

Structural comparisons and redox property of the proteins

Globular proteins usually have highly compact struc-

Table 7 Enthalpy and entropy changes for the electron transfer from ferrocycytochrome b_5 or its P40V mutant to ferricytochrome c at different ionic strengths

I (mmol/L)	ΔH^\ddagger (kJ·mol ⁻¹)		ΔS^\ddagger (J·mol ⁻¹ ·K ⁻¹)	
	WT	P40V	WT	P40V
150	36.7 ± 3.5	41.4 ± 0.7	30.3 ± 12.3	42.0 ± 2.5
350	32.6 ± 1.9	30.2 ± 2.4	2.2 ± 6.4	-9.4 ± 8.2
500	31.1 ± 0.8	30.1 ± 1.0	-8.0 ± 2.8	-14.6 ± 3.5
800	33.6 ± 0.8	35.4 ± 1.5	-5.9 ± 2.8	-2.2 ± 5.2

tures, which might be influenced by the volume change of the side chains introduced by mutation. When proline was replaced by valine, tyrosine or glycine, the changes of volume are +0.012, +0.074, and -0.063 nm³, respectively.³⁷ Furthermore, the Pro40 residue, which locates at the β -turn between α -helix II (residues 32—39) and α -helix III (residues 43—50) in the hydrophobic heme pocket, might serve as a restriction factor in the folding of the protein, owing to its five-member ring side chain. Originally, it was expected that when Pro40 was replaced by another residue, it might result in the elimination of the restriction. This would cause a large change of the polypeptide chain folding. From this point, it would be expected that Pro40 might play an important role in the folding of Cyt b_5 .^{38,39}

However, what struck us most was that the results of UV-visible spectroscopy, circular dichroism and fluorescence spectrum suggested that the substitution of proline by valine does not lead to significant change to the overall protein. In order to provide further structural information on the P40V mutant, the three-dimensional structure of the P40V mutant was determined by X-ray crystallographic analysis. The results show that the secondary structure of the mutant does not differ significantly from that of the wild type protein, and the β -turn in which the Pro40 is located is not eliminated by the mutation. The tertiary structure of the P40V mutant is also very similar to that of the wild type protein and only conformational changes were observed in the local region near the mutation site in the heme pocket. It was found that the C α atom of Val40 moves away from the heme plane by 0.040 nm compared with the position of the C α atom of Pro40 in the wild type protein. Furthermore, the side chain of Val40 points toward the top of the heme and makes van der Waals contacts with the heme (Fig. 1). Interestingly, it is noted that elimination of five-member ring of the proline and moving away of Val40 backbone open a crevice on the

side of the heme pocket, a water molecule (Wat321) is found near the mutation site. This water molecule forms two hydrogen bonds with the amide nitrogen atom of Val40 and the main chain oxygen atom of Glu38, respectively, in addition to a hydrogen bond with a water molecule (Wat322) of the symmetry-related molecule. Therefore, a new hydrogen bond network is formed near the mutation site in the heme pocket. These interactions probably influence the heme conformation and perturb the heme environment.

As an electron transfer protein, the reduction potential is generally regarded as the thermodynamic driving force for the redox reaction. In the biological electron transfer reactions, it is the redox potential difference between the protein partners that makes the electron transfer take place in the correct direction. Thus, it is often desirable to examine redox potential change between a protein and its mutants for exploring the roles played by a particular residue. In previous studies, a large number of theoretical and experimental studies have been focused on the factors affecting the redox potential of the proteins. Taking all these results together, we conclude that at least six major factors contribute to the redox potential of Cyt b_5 : (a) direct perturbations on the heme, including the axial ligand and the interactions between the heme propionates and exogenous ions;^{40,41} (b) perturbations induced by interactions of residues in the proximity of the heme with the prosthetic heme group;^{23,42} (c) changes of the electrostatic potential around the heme-exposed area;¹⁶ (d) alteration of the hydrophobicity of the heme pocket;⁴³⁻⁴⁵ (e) the different heme orientation in the heme pocket of hemoproteins;⁴⁶ (f) the orientation of imidazole planes of axial ligand modulates the redox potential.⁴⁷

In this work, a very interesting result is that the redox potential of the mutant is 40 mV lower than that of the wild type protein. The change from proline to valine is reasonably conservative. Neither the volume nor the

hydrophobicity of the mutated residue was changed much. The X-ray structural analysis confirmed that the overall structure is not affected significantly by this mutation. Therefore, in the case of the P40V mutant, the first three factors discussed above probably exhibit little effect on the redox potential. However, in this mutant, substitution of a valine residue for Pro40 opens a channel for the water molecule to enter the heme pocket and forms a new network of hydrogen bonding. This suggests that the decrease in hydrophobicity of the heme pocket results in the redox potential shift. In the oxidized state of cytochrome proteins, the heme possesses a formal charge of +1, while in the reduced state, the heme possesses a formal charge of zero. Consequently, a hydrophobic environment destabilizes the oxidized state, compared to the reduced state, and results in a relatively higher redox potential. On the other hand, a hydrophilic environment stabilizes the oxidized state leading to a lower redox potential.⁴⁸ Therefore, the reduction of hydrophobicity reasonably accounts for the lower redox potential of the P40V mutant. Earlier, we investigated the effects of the mutations at Phe35, Val45 and Val61 on the redox potential of the proteins.^{42,16,23} It was demonstrated that perturbation of the hydrophobicity of the heme pocket is one of the most important factors contributing to the redox potential alteration. Structural comparisons show that the overall structures of all these mutants are essentially the same as that of the wild type protein. All of these results demonstrate that the redox potential of Cyt *b*₅ could be regulated by hydrophobicity and electrostatic potential of the heme pocket without significantly changing its overall structure.

Protein stability

As mentioned previously, it was expected that substitution of the invariant Pro40 might induce changes in the stability of the protein. Denaturation studies of the P40V mutant towards heat, urea, acid and ethanol did indicate that the mutant was less stable than the wild type protein. We have also used UV-visible, CD, and fluorescence spectroscopy to investigate the unfolding and the refolding processes of wild type Cyt *b*₅ and the P40V mutant that were induced by methanol.²³ These studies reveals that the substitution of valine for proline makes the protein less stable.

Previous studies have shown that there are several factors contributing to the stability of protein.⁴⁹ Because

Pro40 is in direct van der Waals contact with the heme, factors such as hydrophobic effects, hydrogen bonds, and local polarity must also be considered for their importance in the stability of the protein. Crystallographic analysis of the P40V mutant demonstrates that substitution of this proline residue by valine opens a crevice on the side of the heme pocket that may function as a channel for solvent access to the heme center. A trapped water molecule in the heme pocket also increases the hydrophilicity of the active site. These local perturbations make hydrophobic residues in proximity of this position more exposed to the solvent. These factors should also contribute to the decreased stability of the P40V mutant. The decreased stability caused by opening of a water channel was also observed in the Cyt *b*₅ V61H mutant.¹⁶

In general, hydrogen-bonding interactions are usually conducive to the stability of proteins. In the structure of Cyt *b*₅ P40V mutant, although two hydrogen bonds are formed in the heme pocket from a new water molecule to protein main chain atoms, this stabilization factor is not sufficient to compensate for the destabilization due to decrease in hydrophobicity of the heme pocket and the exposure of the heme to the solvent; thus, the P40V mutant is less stable than wild type Cyt *b*₅.

On the basis of the above discussion, it is evident that substitution of Pro40 led to local structural perturbation and destabilization of the heme binding in these variants. As we mentioned before, three mutant genes P40V, P40G and P40Y were successfully constructed; however, only the P40V gene was successfully expressed into holoprotein. Protein electrophoresis results showed that a clear band of the apo-cytochrome *b*₅ appeared in the P40G and P40Y expressed protein spectra. One of the reasons for those variants not successfully expressed could be that the structural perturbations that were introduced by some residues in the heme pocket, cause the association for the heme to be diminished to such extent that the holoproteins could not be formed. For the P40V mutant, although the holoprotein has been obtained, however, significant decreases of the stability are also observed.

Binding and electron transfer

To assess the effect of the substitution of valine for Pro40 on the function of Cyt *b*₅, binding and electron transfer between Cyt *b*₅ and Cyt *c* were studied. The

binding constant of Cyt b_5 to Cyt c was almost the same as that for the wild type protein. However, the electron transfer rates decreased significantly due to the mutation. Thus, it was showed that there was no direct relationship between the binding constant and electron transfer. This may be attributed to dynamic nature of electron transfer process, which is related to the association and successive electron transfer of the two protein partners within a short time, while the binding constants exhibit the binding strength in terms of a thermodynamic equilibrium. Perhaps, the most stable conformation for binding is not necessarily the most favorable conformation for the electron transfer.

As we mentioned above, the redox potential of the electron transfer protein can be regarded as the thermodynamic driving force for the reaction. In general, the more negative the redox potential of Cyt b_5 mutant, the faster electron transfer should occur. However, it was not the case in the P40V mutant. Although its redox potential is about 40 mV lower than that of the wild type protein, the higher driving force of Cyt b_5 P40V-Cyt c system should have higher electron transfer rate compared with the wild type Cyt b_5/c system. Actually, its electron transfer rate was only three fifths of that of the wild type protein at ionic strength of 150 mmol/L. It is evident that redox potential is not the only factor influencing the electron transfer rate. Previous studies have demonstrated that electron transfer is modulated by several factors, including driving force, orientation, distance, intervening media and in some cases dynamics.⁵⁰ Then the question which can be asked is what the important factors contributing to such rate behaviors here are?

As shown in Fig. 9, electron transfer rates of the wild type and the P40V mutant are strongly dependent on the ionic strength, which suggests that electrostatic interactions play an important role in the electron transfer. However, the fitted curves for electron transfer for the two proteins are almost parallel. This phenomenon is different from the results of other mutants. For example, when Glu44 or Glu56 of Cyt b_5 or Lys32 of Cyt c were replaced by Ala, Ala, and Gln, respectively, the differences in rate constants were most pronounced at low ionic strength and were minimal at higher ionic strength.^{1,37,51} In contrast, the difference in the rate constants between the wild type and the P40V mutant was independent on ionic strength. This kind of independence reveals that here the structural perturbations also play roles in electron transfer

between Cyt b_5 P40V mutant and Cyt c . This result combined with previous studies mentioned above indicates that both electrostatic interactions and structural perturbations are major factors contributing to the electron transfer of the P40V mutant with Cyt c .

Substitution of proline by valine does not introduce a change in charge, so those electrostatic interactions are not likely to be disturbed. However, owing to the great structural complexity of proteins, the conformational perturbations caused by the mutation must be considered. In wild type Cyt b_5 , Pro40 is a member of the hydrophobic patch residues, which is partially exposed to solvent at the surface of Cyt b_5 .^{11,12} In addition, this residue is located at the rim of the heme hydrophobic pocket. Any subtle conformational change around Pro40 would perturb the heme propionate and the negatively charged area at surface (including Glu44, *etc.*) proposed to be involved in the interaction with Cyt c . Although replacement of proline by valine did not induce large changes in the overall structure, the local conformational changes influence the interface between Cyt b_5 and Cyt c , consequently, decreases the electron transfer rate. The driving force of the P40V mutant is favorable to the electron transfer, however, it can not compensate for the effect of unfavorable conformational changes, so the ultimate result is the decrease of the electron transfer rate.

Conclusions

In this paper, The structure, properties and function of Cyt b_5 P40V mutant have been investigated. For the P40V mutant protein the redox potential and stability towards heat, denaturant and organic solvent have been dramatically changed, and its electron transfer reaction with Cyt c significantly affected. X-ray structural analysis shows that on the whole, the overall structure of the mutant is less affected, while the local conformational changes have been observed. It is the local conformation perturbations that cause the dramatic change in the protein stability and electron transfer rate between Cyt b_5 and Cyt c . It is demonstrated that invariant proline-40 is essential to maintaining Cyt b_5 's stability and its electron transfer with Cyt c . Moreover, mutations at Val61, Val45 and Phe35, which are also invariant or highly conserved residues in the heme pocket of Cyt b_5 , exhibit the similar behaviors.^{16,24,33} From these structure-based functional analysis studies, it is becoming clearer that

functional changes of proteins, especially in the globular proteins like Cyt b_5 , do not necessarily originate from or require large overall structural alterations. Only perturbations on the local conformations are sufficient to induce significant changes in protein properties and functions of Cyt b_5 . It really gives us a good example in understanding that proteins are so well-structured and architected in most cases, especially in the globular proteins, and the exquisite organization, assembling and the extent of matching are so precise and wonderful. Good fidelity of biological activity is very much dependent on just those subtle conformational changes (sometime, it is alteration of only few tenths of Angstroms). It also provides us a detailed molecular base for understanding why point mutations and structural transformations that occurred in normal protein would cause a variety of physiological dysfunction.⁵²⁻⁵⁴

Acknowledgments

We are grateful to Prof. Li-Wen Niu, Prof. Mai-Kun Teng and Dr. Xue-Yong Zhu of the University of Science and Technology of China for their support and help with the X-ray data collection.

References

- Sun, Y. L.; Wang, Y. H.; Yan, M. M.; Sun, B. Y.; Xie, Y.; Huang, Z. X.; Jiang, S. K.; Wu, H. M. *J. Mol. Biol.* **1999**, *285*, 347.
- Rodgers, K. K.; Pochapsky, T. C.; Sligar, S. G. *Science* **1988**, *240*, 1657.
- Mauk, M. R.; Reid, L. S.; Mauk, A. G. *Biochemistry* **1982**, *21*, 1843.
- Poulos, T. L.; Mauk, A. G. *J. Biol. Chem.* **1983**, *258*, 7369.
- Tamburini, P. P.; White, R. E.; Schenkman, J. B. *J. Biol. Chem.* **1985**, *260*, 4007.
- Stayton, P. S.; Poulos, T. L.; Sligar, S. G. *Biochemistry* **1989**, *28*, 8201.
- Bernardi, P.; Azzone, G. F. *J. Biol. Chem.* **1981**, *256*, 7187.
- Lederer, F. *Biochimie* **1994**, *76*, 674.
- Salemme, F. R. *J. Mol. Biol.* **1976**, *102*, 563.
- Northrup, S. H.; Thomasm, K. A.; Miller, C. M.; Barker, P. D.; Eltis, L. D.; Guillemette, J. G.; Inglis, S. C.; Mauk, A. G. *Biochemistry* **1993**, *32*, 6613.
- Durley, R. C.; Mathews, F. S. *Acta Crystallogr.* **1996**, *D52*, 65.
- Wu, J.; Xia, Z. X.; Wang, Y. H.; Wang, W. H.; Xue, L. L.; Xie, Y.; Huang, Z. X. *Proteins: Struct., Funct., Genet.* **2000**, *40*, 249.
- Ozols, J. *Biochim. Biophys. Acta* **1989**, *997*, 121.
- Funk, W. D.; Lo, T. P.; Mauk, M. R.; Brayer, G. D.; MacGillivray, R. A.; Mauk, A. G. *Biochemistry* **1990**, *29*, 5500.
- Zoller, M. J.; Smith, M. *Methods Enzymol.* **1983**, *100*, 458.
- Xue, L. L.; Wang, Y. H.; Xie, Y.; Yao, P.; Wang, W. H.; Qian, W.; Huang, Z. X.; Wu, J.; Xia, Z. X. *Biochemistry* **1999**, *38*, 11961.
- Mathews, F. S.; Levine, M.; Argos, P. *J. Mol. Biol.* **1972**, *64*, 449.
- Otwinowski, Z.; Minor, W. *Methods Enzymol.* **1997**, *276*, 307.
- Brunger, A. T. *X-PLOR: A System for X-Ray Crystallography and NMR*, Version 3.1, Yale University Press, New Haven, **1992**.
- Goussel, A.; Cambillau, C. *TURBO-FRODO*, Silicon Graphics Partner Geometry Dictionary, Silicon Graphics Inc (eds.), **1991**.
- Yao, P.; Wu, J.; Wang, Y.-H.; Sun, B.-Y.; Xia, Z.-X.; Huang, Z.-X. *Eur. J. Biochemistry*, revised.
- Brunger, A. T.; Adams, P. D.; Clore, G. M.; Delano, W. L.; Gros, P.; Kunstleve, R.; Jiang, J. S.; Kuszewski, J.; Nilges, N.; Pannu, N. S. *Acta Crystallogr.* **1998**, *D54*, 905.
- Wang, Z.-Q.; Wang, Y.-H.; Qian, W.; Wang, W.-H.; Chunyu, L.-J.; Xie, Y.; Huang, Z.-X. *J. Protein Chem.* **1999**, *18*, 547.
- Wang, Z. Q.; Wang, Y. H.; Wang, W. H.; Xue, L. L.; Wu, X. Z.; Xie, Y.; Huang, Z. X. *Biophys. Chem.* **2000**, *83*, 3.
- Ozols, J.; Strittmatter, P. *J. Biol. Chem.* **1964**, *239*, 1018.
- Margoliash, E.; Frohwirt, N. *Biochem. J.* **1959**, *71*, 570.
- Yao, P.; Wang, Y.-H.; Sun, B.-Y.; Xie, Y.; Hirota, S.; Yamauchi, O.; Huang, Z.-X. *J. Biol. Inorg. Chem.*, **2002**, *7*, 375.
- Ramachandran, G. N.; Sasisekharan, V. *Adv. Protein Chem.* **1968**, *28*, 283.
- Luzzati, P. V. *Acta Crystallogr.* **1952**, *5*, 802.
- Newbold, R. J.; Hewson, R.; Whitford, D. *FEBS Lett.* **1992**, *314*, 419.
- Vergeres, G.; Chen, D. Y.; Wu, F. F.; Waskell, L. *Arch. Biochem. Biophys.* **1993**, *305*, 231.
- Hewson, R.; Newbold, R. J.; Whitford, D. *Protein Eng.* **1993**, *6*, 953.
- Yao, P.; Wang, Y.-H.; Sun, Y.-L.; Huang, Z.-X.; Xie, Y.; Xiao, G.-T. *Protein Eng.* **1997**, *10*, 575.

- 34 Storch, E. M.; Daggett, V. *Biochemistry* **1996**, *35*, 11596.
- 35 Erman, J. E.; Vitello, L. B. *J. Biol. Chem.* **1980**, *255*, 6224.
- 36 Mauk, A. G.; Mauk, M. R.; Moore, G. R.; Northrup, S. H. *J. Bioenerg. Biomembr.* **1995**, *27*, 311.
- 37 Caffrey, M. S. *Biochimie* **1994**, *76*, 622.
- 38 Nall, B. T.; Osterhout, J. J.; Ramdas, L. Jr. *Biochemistry* **1988**, *27*, 7310.
- 39 White, T. B.; Berget, P. B.; Nall, B. T. *Biochemistry* **1987**, *26*, 4358.
- 40 Sligar, S. G.; Egeberg, K. D. *J. Am. Chem. Soc.* **1987**, *109*, 7896.
- 41 Wang, Y.-H.; Cui, J.; Sun, Y.-L.; Yao, P.; Zhuang, J.-H.; Xie, Y.; Huang, Z.-X. *J. Electroanal. Chem.* **1997**, *428*, 39.
- 42 Yao, P.; Wang, Y.-H.; Xie, Y.; Huang, Z.-X. *J. Electroanal. Chem.* **1998**, *445*, 197.
- 43 Langen, R.; Brayer, G. D.; Berghuis, A. M.; McLendon, G.; Sherman, G.; Warshel, A. *J. Mol. Biol.* **1992**, *224*, 589.
- 44 Zhou, H. X. *J. Am. Chem. Soc.* **1994**, *116*, 10362.
- 45 Quinn, R.; Mercer-Smith, J.; Burstym, J. N.; Valentine, J. S. *J. Am. Chem. Soc.* **1984**, *106*, 4136.
- 46 Walker, F. A.; Huynh, B. H.; Scheidt, W. R.; Osvath, S. R. *J. Am. Chem. Soc.* **1986**, *108*, 5288.
- 47 Walker, F. A.; Emrick, D.; Rivera, J. E.; Hanquet, B. J.; Buttlare, D. H. *J. Am. Chem. Soc.* **1988**, *110*, 6234.
- 48 Caffrey, M. S.; Cusanovich, M. A. *Biochim. Biophys. Acta* **1994**, *1187*, 277.
- 49 Sandberg, W.; Terwillger, T. *Science* **1989**, *245*, 54.
- 50 Marcus, R. A.; Sutin, N. *Biochim. Biophys. Acta* **1985**, *811*, 265.
- 51 Guillemette, J. G.; Barker, P. D.; Eltis, L. D.; Lo, T. P.; Smith, M.; Brayer, G. D.; Mauk, A. G. *Biochimie* **1994**, *76*, 592.
- 52 Wallace, C. D. *Annu. Rev. Biochem.* **1992**, *61*, 1175.
- 53 Prusiner, S. B. *TIBS* **1996**, *21*, 482.
- 54 Ng, S. B. L.; Doig, A. J. *Chem. Soc. Rev.* **1997**, *26*, 425.

(E0205062 PAN, B. F.; DONG, H. Z.)